VIBRATION-BASED DAMAGE DETECTION FOR TIMBER STRUCTURES IN AUSTRALIA

B. Samali*, J. Li*, U. Dackermann* and F. C. Choi*

University of Technology Sydney, Australia

* Centre for Built Infrastructure Research (CBIR), University of Technology Sydney, Australia

ABSTRACT

The use of non-destructive assessment techniques for evaluating structural conditions of aging infrastructure, such as timber bridges, utility poles and buildings, for the past 20 years has faced increasing challenges as a result of poor maintenance and inadequate funding. Replacement of structures, such as an old bridge, is neither viable nor sustainable in many circumstances. Hence, there is an urgent need to develop and utilize state-of-the-art techniques to assess and evaluate the "health state" of existing infrastructure and to be able to understand and quantify the effects of degradation with regard to public safety. This paper presents an overview of research work carried out by the authors in developing and implementing several vibration methods for evaluation of damage in timber bridges and utility poles. The technique of detecting damage involved the use of vibration methods, namely damage index method, which also incorporated artificial neural networks for timber bridges and time-based non-destructive evaluation (NDE) methods for timber utility poles. The projects involved successful numerical modeling and good experimental validation for the proposed vibration methods to detect damage for simple beams subjected to single and multiple damage scenarios and was then extended to a scaled timber bridge constructed under laboratory conditions. The time-based NDE methods also showed promising trends for detecting the embedded depth and condition of timber utility poles in early stages of that research.

INTRODUCTION

Australia has been, historically, blessed with plentiful supplies of native hardwood timbers. Such timber is of both strong and durable species. As a result, these materials were heavily used during the early European settlement since 1788, for developing transport links such as wharf and bridge structures. Later, timber was used for utility poles for transmission of electricity and communication lines (Crews, 2008).

Recent surveys have shown that there are approximately 29,000 timber bridges in Australia, of which many are still in service despite being degraded or in structurally weakened condition (DoTaRS, 2003). The enormous number of timber bridges, which form a significant portion of bridges in Australia (total is in excess of 40,000), reflects the importance of these structures to the country's economic growth and the daily life of many Australians. In addition, these bridges are highly valued, not just for economic reasons, but also for the social and historical value placed on them by rural communities.

The Department of Transport and Regional Services Australia (DoTaRS, 2003) has estimated that a third of timber bridges are in excess of 50 years old. These bridges are located mainly on regional roads, owned and maintained by local government agencies. Due to lack of funds and engineering expertise, it is not easy to undertake thorough condition assessment of these bridges, which are often functionally obsolete and structurally deficient.

Due to their age and unknown "health" condition, it is extremely crucial for asset managers to have a reliable tool for monitoring and evaluation of the state of health of their bridge stocks in order to carry out timely maintenance and repair/replacement, and therefore ensure the safety of public as well as preserve these heritage-valued structures for the country (McInnes, 2005).

Another important component of Australia's infrastructure is timber utility poles. According to Nguyen et al. (2004) and Francis and Narton (2006), there are nearly seven million utility poles in the current network, of which around five million timber poles are used for distribution of power and communications. The utility pole industry in Australia spends about $40~50 million annually on maintenance and asset management to avoid failure of the utility lines, which is very costly and may cause serious consequences. Each year, about 30,000 electricity poles are replaced in the eastern states of Australia, despite the fact that up to 80% of these poles are still in a very good serviceable condition. For timber utility poles, investigation of asset management systems for the power distribution industry shows that the design and assessment methods, which form traditional industry practices in Australia, are imprecise and often unreliable. Assessment techniques are required to maintain a high level of reliability against pole failure. There is a need for a simple, reliable and effective tool for determination of embedded length and condition of timber utility poles in service.

This chapter reports on research work carried out by the authors in development and implementation of vibration-based methods for evaluation of damage and state of health of timber structures. For damage detection and damage severity estimation, a modified damage index method (MDI) has been developed for dealing with timber beam-like structures, and a damage index method for plate-like structures (DI-P) was proposed for timber bridges and timber decks. Both the methods were formulated based on modal strain energy. In addition to numerical investigations using finite element models, the researchers carried out experimental studies on timber beams and a laboratory prototype timber bridge subjected to single- and multiple-damage scenarios. To enhance the damage detection results and to overcome shortcomings of the proposed modal-strain-energy-based methods, integration of artificial neural networks (ANNs) in form of a network ensemble was also proposed in damage localization and severity estimation. The research and development of damage detection in timber utility poles including use of non-destructive evaluation (NDE) techniques for determination of condition and underground depth of embedded timber poles in-service is also briefly reported in this chapter.

LITERATURE REVIEW

State-of-the-Art in Damage Detection for Timber Structures

Timber/wood has been used extensively as building material for centuries. The degradation of structural members of timber may be due to several causes, such as biotic degradation and physical degradation. It is, therefore, important to perform periodical condition assessment and evaluation on the structures to determine the extent of deterioration for a proper maintenance schedule. Often the problems in wood/timber structures do not lie in the effectiveness of preserving systems of the material itself but in not having the correct tools necessary to locate deterioration (Duwadi et al., 2000). Thereby, it delays application of remedial treatments to prevent further degradation in the structures. The current state-of-the-art for in-situ condition assessment and evaluation of timber consists of several steps either through non-destructive, destructive or semi-destructive means as briefly listed in Table 1 (Kasal, 2008). A wide variety of techniques being used to verify deterioration in timber members can be found in Ross et al. (2006).

Table 1. Classification Of Methods For In-Situ Timber Evaluation (Kasal, 2008)

Method		
NON-DESTRUCTIVE	DESTRUCTIVE	SEMI-DESTRUCTIVE
Visual inspection	Specimen extraction	Resistance drilling
Stress and acoustic waves	Full-member tests	Core drilling
Moisture contentmeasurements	Standard tests of mechanical properties	Tension micro-specimens
Radiography		Pin penetration resistance
Computer tomography		Other non-conventional methods
Species determination		
Dendrochronology		

It is quite obvious that destructive tests impose several disadvantages such as complete loss of the element of interest. For semi-destructive methods, they are non-destructive with respect to the member of interest, but are destructive with respect to the extracted specimen itself. Hence, non-destructive methods are widely used by engineering practitioners lately, as these methods do not alter much the tested member material properties. However, many non-destructive techniques (NDTs) are mostly used on small and accessible areas. It is time consuming to perform them on large timber structures like timber bridges, and it is also costly. This led to research on global methods, which would be able to reduce testing time, the cost involved and disruption to traffic flow. If necessary, the global methods can be combined with other more localized NDE methods for evaluating damage details.

Over the last few decades, many methods assessing global structural integrity for timber structures have been developed. Some recent works have focused on using vibration techniques, which are non-destructive in nature, to assess the in-service stiffness of timber structures like short-span timber bridges and floor systems within buildings. For timber structures, the focus of developments on vibration techniques has been on assessing the condition of wood in-service based on techniques that evaluate individual members and small

area defects within a wood member. The basis of vibration-based methods is that any changes in the physical properties of wood such as mass, damping and stiffness, will in turn alter its dynamic characteristics, namely, natural frequency, damping ratio and mode shape.

Peterson et al. (2001a,b) reported on adopting the damage index method for one-dimensional (1-D) systems that utilizes modal strain energy before and after damage for identifying local damage and decay in timber beams using the first two flexural modes. The researchers also mentioned that the mode shapes to be used in the damage localization algorithm should be selected according to the location of damage. The method is quite promising for single-damage scenarios but it does not work well for two-damage scenarios in a timber beam. Furthermore, the results showed that the method is quite mode dependant.

Morison et al. (2002) presented the possibility of extending global testing methods, specifically, impact testing, for determining if damage in the form of decay is present in timber bridges. The project also intended to provide cost and time savings over existing methods of inspecting timber bridges. The method is to correlate the first natural frequency (fundamental frequency) with stiffness characteristics of timber bridge stringers (girders) using an algorithm derived from a partial differential equation governing the transverse vibration of a simple flexural beam. However, the largest obstacles encountered in this study were the actual boundary conditions of a bridge in the field, which are difficult to determine. Similar efforts were extended by Morison et al. (2003) in investigating dynamic characteristics of timber bridges using several existing methods such as damage index derived from estimated and measured curvature and flexibility influence coefficient estimated by the direct current (DC) value of the frequency response function (FRF) matrix. The results showed that the broadband curvature method was successful in showing a difference between the original state and the damaged state. However, it is far from a quantitative prediction of damage. While the flexibility influence coefficient method was able to show a change in the system when a weaker stringer replaces an original one, it failed to identify which stringer was replaced. Similar work was reported by Wang et al. (2005).

Hu and Afzal (2006) used a damage indicator for the detection of single- and two-damage cases of timber beams. The damage indicator is derived from the difference of the mode shapes before and after damage. The indicator is then expressed using discrete Laplace transform and finally normalized statistically in space. The method using either first or second modes successfully identified single artificial defect at different locations and a two-damage case with equal spacing and similar level of damage severity. However, the method is incapable of evaluating quantitatively the severity of damage. In addition, the method found difficulty in generating higher mode shapes as well as the combination of first and second modes. The damage indicator was further sensitive to different damage locations and different modal orders. The results of this study were based on 43 impact points for each set of data from the modal tests, which may be too time consuming and, hence, not cost effective.

Muller (2008) presented a paper describing the application of ground penetrating radar (GPR) technique to detect defects within the timber superstructure of the Hornibrook Highway Bridge. The author found that GPR was successful in detecting, locating and estimating the extent and severity of girder defects on the bridge in around a fifth of the time and cost of the traditional approach of “visual inspection plus test drilling.” Furthermore, the ability of GPR to locate isolated defects led to numerous defects being found that would have gone undetected based on the traditional visual inspection or targeted test drilling.

Damage Detection utilizing Artificial Neural Network Techniques

In recent years, the use of Artificial Neural Networks (ANNs) in structural damage detection has gained momentum. ANNs are artificial intelligence that simulate the operation of the human brain. They are composed of a large number of highly interconnected processing elements, which are analogous to neurons and are tied together with weighted connections that represent synapses. The key element of ANNs is that they learn by example and not by following programming rules. Once trained, they are capable of pattern recognition and classification and are robust in the presence of noise. These characteristics make ANNs powerful complementary tools in vibrational damage identification. With the use of ANNs, some critical issues in traditional damage detection methods can be overcome and damage detection accuracy and reliability greatly improved.

The first researchers to introduce ANN to vibration-based damage detection in civil structures were Wu et al. (1992). Their paper from 1992, investigates the feasibility of ANN in structural damage detection; Fourier spectrum recordings of an experimental three-storey frame structure were used as ANN inputs to detect damage. The researchers found that the network was successful in identifying the damage condition of each member in the structure and concluded that "the use of neural networks for structural damage assessment is a promising line of research."

Sahin and Shenoi (2002) used changes in natural frequencies and curvature mode shapes as input features for ANNs for location and severity prediction of numerical and experimental damage in cantilever steel beams. From the network predictions, they found that the reduction in natural frequency provides the necessary information for the existence and severity of damage, however, differences in curvature mode shapes severed as better indicator in the location predictions.

Many successful applications have also been reported on multi-stage damage assessment methods that incorporate artificial intelligence techniques. Ko et al. (2002) developed a three-stage identification scheme, which was applied to numerical simulations of the Kap Shui Mun cable-stayed bridge in Hong Kong. In the first stage, auto associative neural networks are fed with natural frequencies to identify the existence of damage. This was followed by a combination of modal curvature index and modal flexibility index to identify the damage area. In the third stage, ANNs were used to determine specific damage member(s) and damage severity.

Lee and Yun (2006) presented a two-step damage identification strategy and demonstrated the method on numerical data and field test data of the old Hannam Grand Bridge in Seoul, Korea. First, the DI method was used to screen potentially damaged members and then, neural networks were trained with mode shape differences between before and after damage to assess the defects. They found that while the damage screening of the first step gave many false damage alarms, the damage assessment results using neural networks showed good estimates for all damage cases.

Another multi-stage damage assessment approach was proposed by Bakhary et al. (2007), who used substructure techniques together with a two-stage ANN model to detect single- and multiple-damage scenarios. The method was successfully demonstrated on numerical simulations of a two-span concrete slab.

An extension to ANNs are neural network ensembles (also referred to as committees or classifier ensembles), which are a hierarchy of networks that are trained independently for the same task and whose outcomes are fused at different stages by ensemble networks. These neural network committees were observed to perform better than the best network used in isolation (Perrone and Copper, 1993) and are currently used in many fields of research.

The idea of multi-stage network training was first employed in the area of vibration-based damage detection by Marwala and Hunt (1999). The researchers applied a two-stage neural network ensemble to numerically simulated cantilever beam data, with one network trained with frequency energies, which are integrals of the real and imaginary components of the frequency response functions over various frequency ranges, and another network trained by using the first five flexural mode shape vectors. The authors found that the ensemble gave a mean error of 7.7% compared to 9.5% and 9.78%, respectively, of the individual networks. In an extension to this work, Marwala (2000) presented a committee of neural network approach, which employs frequency response functions (FRFs), modal properties (natural frequencies and mode shapes), and wavelet transform (WT) data of numerical and experimental steel seam-welded cylindrical shells. The data were separately fed to three neural networks, which were later combined in a committee network. It was found that the committee identified the damage cases better than the three approaches used individually.

Vibration-Based Assessment Work Undertaken at the Centre for Built Infrastructure Research at UTS

In the authors' research group (CBIR), studies on vibration-based assessment methods for timber structures started in early 2000. A simple dynamic testing method, based on structural frequency shift (SFS), was developed by Samali et al. (2002, 2003a,b) (related work is also published in Li et al., 2004; Crews et al., 2004; and Benitez and Li, 2002) to evaluate the global stiffness and strength of in-service timber bridges. This dynamic method is generally proven to be easily performed and cost effective. In addition, the operators are not required to have high skills and can be easily trained on the job to perform the dynamic timber testing. The method has been successfully used to undertake field-testing of more than 600 timber bridge spans across New South Wales (NSW). The testing procedure involves the attachment of accelerometers underneath the bridge girders and exciting the bridge with a modal hammer with and without extra mass blocks at mid-span of the bridge. In order to refine the method and to further reduce cost and testing time as well as evaluate some of the practical issues during the field testing, a project was initiated to investigate the effects of using alternative mass forms, such as use of a trailer to replace currently used mass blocks, and adding mass at locations other than mid-span, on the bridge vibrations and subsequent integrity assessment (Li et al., 2005). The authors have progressively expanded the research work to also detect the location of damage and to evaluate damage severity. The modal-strain-energy-based damage index method for beam-like structures (DI) and its modified version (MDI), as well as damage index (DI) method for plate-like structures (DI-P) form the basis for the developed location and severity identification methods. For improved damage evaluation, artificial neural network techniques were introduced in the detection procedures. Indices of the DI method and compressed frequency response functions are used as input parameters for neural network training. Selected publications are listed in (Choi, 2007; Choi et al., 2007; Choi et al.,

2008a,b; Li et al., 2007; Samali et al., 2009; Dackermann et al., 2008a,b, 2009). Furthermore, the group also started another research project using vibration-based methods to estimate embedded length in soil for timber utility poles as well as determining their structural conditions (Zad, 2009). Some of the research outcomes that deal with the identification of damage locations and severities on timber beams and timber bridge decks are presented in the following sections.

DAMAGE DETECTION ON TIMBER BEAM STRUCTURE

Timber Beam Structure

Pin-pin supported timber beams were chosen to verify the developed methods on a simple structure. The timber beams are intended to represent scaled girders of typical timber bridges in Australia. The scaling for the beams was based on dynamic similitude of the girders in terms of their first natural frequencies, which usually range from 5 to 20 Hz.

Laboratory Timber Beam

Experimental timber beams were set up and tested in the Structures Laboratory of the University of Technology Sydney (UTS). The beams were of treated radiata pine sawn timber, measuring nominal dimensions of 45 mm by 90 mm in cross-section with a span length of 4,500 mm. The modulus of elasticity (MOE) of the beams was about 12GPa obtained from four-point bending tests. The experimental set up is displayed in Figure 1(a).

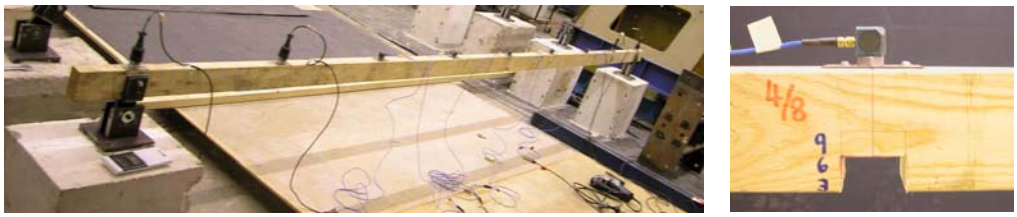

(a) (b)

Figure 1. (a) Experimental test set up and (b) medium-size damage (27 mm × 45 mm) of timber beam

Two laboratory timber beam structures were tested and inflicted with various types of damage. Single- and multiple-damage scenarios with different damage locations and severities were investigated. All damage scenarios consisted of a rectangular opening from the soffit of the beam, located at 1/4, mid-span (1/2), and 3/4 of the span length to simulate pockets of rot. Damage descriptions are as follows, L, M, and S are used to denote “light,” “medium,” and “severe” damage, respectively. All inflicted damage occupied 1% of the total span length (45 mm) and consisted of 10%, 30%, or 50% of the beam depth, designated as damage cases L, M, and S, respectively. The 10%, 30%, and 50% of the beam depth cut in cross section correspond to losses of sectional “I” (moment of inertia) of 27.1%, 65.7%, and 87.5%, respectively. The cases described in this chapter are listed in Table 2. A medium-size damage is displayed in Figure 1 (b).

Table 2. Dimensions of Damage Inflicted in Timber Beams

Damage Case	Damage Scenario	Location per 8^{th} of span length	Length l (mm)	Depth h (mm)	% reduction of "I"
1	4L	4	45	9	27.1
2	4M	4	45	27	65.7
3	4S	4	45	45	87.5
4	4S6L	4, 6	45	45, 9	87.5, 27.1
5	4S6S	4, 6	45	All 45	All 87.5

To obtain the modal parameters of the beam, experimental modal testing and analysis was performed. In modal testing, the beams were excited by an impact hammer, and the acceleration responses were measured by nine equally spaced piezoelectric accelerometers. The time history signals of the hammer and the acceleration responses were first amplified by signal conditioners and then recorded by a data acquisition system. The sampling rate was set to 10,000 Hz for a frequency range of 5,000 Hz and 8,192 data points, thus giving a frequency resolution of 0.061 Hz. The time history data were then transformed into the frequency spectra using fast Fourier transform (FFT). By dividing the frequency spectra signals of the response data by the frequency spectra of the excitation data, the frequency response functions (FRFs) were obtained. The first five flexural modes of the beam were identified by performing modal analysis utilizing the leading software from LMS (LMS CADA-X). The corresponding mode shapes were mass normalized, and in order to enhance the quality and effectiveness of damage identification, the mode shape vectors were reconstructed from nine to 41 data points utilizing cubic spline interpolation techniques. The experimental modal testing set up and modal analysis procedures are shown in Figure 2.

Numerical Timber Beam Model

For damage severity estimation, artificial neural network techniques are employed. To generate patterns for the training of the networks, a numerical model of the timber beam structure is created using the finite element analysis package ANSYS. The dimensions and material properties of the pin-pin supported beam model comply with the specifications of the experimental beams. The cross-section is modeled with 20 elements across the height and four elements along the width. The longitudinal direction of the model is divided into 201 nodes and 200 elements. Seven different damage locations with spacings of 562.5 mm ($1/8^{th}$ of the span length) are considered. The damage locations ("1" to "7") are displayed in Figure 3(a). For each of these locations, five different damage severities, with cuts of 10%, 20%, 30%, 40% and 50% of the beam depth are investigated, generating a total of 35 different damage cases. All inflicted damage are 45 mm in length and 9 mm, 18 mm, 27 mm, 36 mm and 45 mm in height, respectively. This corresponds to 27.1%, 48.8%, 65.7%, 78.4% and 87.5% loss of I. Damage is modeled by rectangular openings from the soffit of the beam along the span length. A medium-size damage is depicted in Figure 3(b).

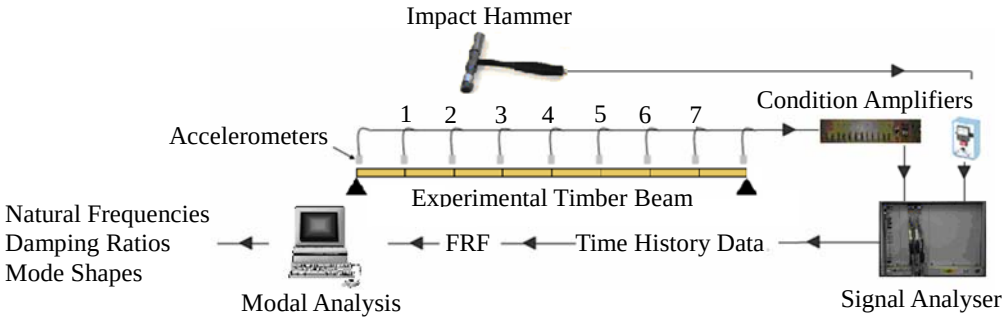

Figure 2. Schematic diagram of experimental modal testing and analysis

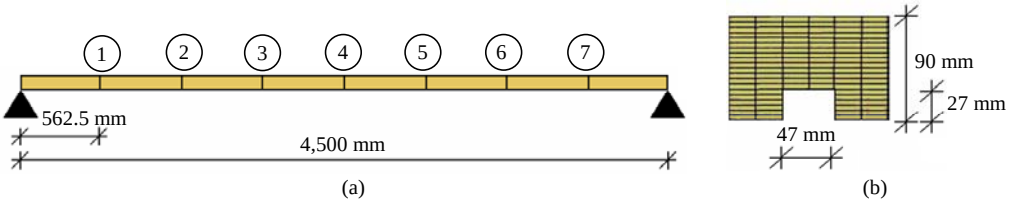

Figure 3. Finite element modeling of (a) pin-pin supported timber beam and (b) medium-size damage

Using the modal analysis module in ANSYS, the first five flexural mode shapes are extracted. To synchronise the numerically obtained data with the experimental data, the mode shape vectors are reduced from 201 data points to nine points, representing the nine measurement sensors of the experimental test set up. Subsequently, the mode shape vectors are again reconstructed from nine to 41 data points, utilizing cubic spline interpolation techniques.

Damage Localization Utilizing MDI Method

Derivation of MDI Method

The damage index (DI) method developed by Kim and Stubbs (1995) was adopted and modified (named as modified damage index (MDI)) to locate damage. The MDI method is based on relative differences in modal strain energy between an undamaged structure and that of the damaged structure. The modal strain energy utilizes mode shape curvature in the algorithm to calculate the damage index for the j^{th} element and the i^{th} mode, β_{ij}, as given below.

$$\beta_{ij} = \frac{\int_j \left\{\phi_i''^{*}(x)\right\}^2 dx \int_0^L \left\{\phi_i''(x)\right\}^2 dx}{\int_j \left\{\phi_i''(x)\right\}^2 dx \int_0^L \left\{\phi_i''^{*}(x)\right\}^2 dx} \quad (1)$$

In Eqn (1), the terms ϕ_i"(x) or ϕ_i"*(x) are normalized mode shape curvature coordinates. The curvature is normalized with respect to the maximum value of the corresponding mode for each mode of a beam structure. The normalized curvature used in the MDI method is shown to perform better in damage localization compared to its original formulae, where curvature was not normalized (Kim and Stubbs, 1995). The asterisk denotes the damage cases. For the original damage index method, although mode shape vectors have been mass normalized, the mode shape curvatures used for the damage index calculation are not normalized. Values of mode shape curvature are dependant on the shapes of each individual mode shape. Instead of reflecting the changes in the curvature due to damage, the summation of non-normalized mode shape curvatures will distort the damage index in favor of higher modes, which results in false damage identifications. The modified damage index (MDI) method introduced above overcomes the problem by normalizing mode shape curvatures with respect to the maximum norm of each mode shape curvature. To account for all available modes, *NM*, the damage indicator value for a single element *j* is given as

$$\beta_j = \frac{\sum_{i=1}^{NM} Num_{ij}}{\sum_{i=1}^{NM} Denom_{ij}} \tag{2}$$

where Num_{ij} = numerator of β_{ij} and $Denom_{ij}$ = denominator of β_{ij} in Eq. (1), respectively. Transforming the damage indicator values into the standard normal space, the normalized damage index Z_j is obtained

$$Z_j = \frac{\beta_j - \mu_{\beta_j}}{\sigma_{\beta_j}} \tag{3}$$

where $\mu_{\beta j}$ and $\sigma_{\beta j}$ are the mean and standard deviation of β_j values for all j elements, respectively.

The estimation of the damage severity for element *j* is expressed by equation

$$\alpha_j = 1 - \frac{1}{\beta_j} \tag{4}$$

with α_j being the severity estimator.

A judgment-based threshold value is selected and used to determine which of the j^{th} elements are possibly damaged, which in real applications is left to the user to define based on what level of confidence is required for localization of damage within the structure.

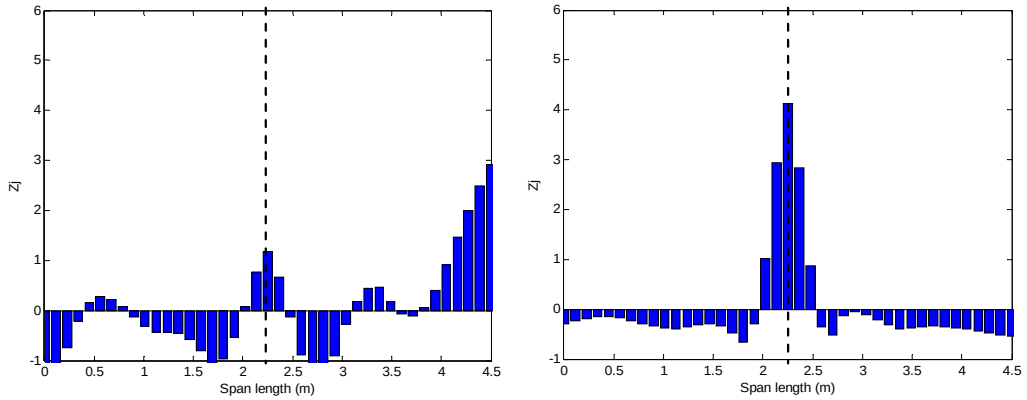

(a) 4L (b) 4S

Figure 4. Damage localization for single-damage cases

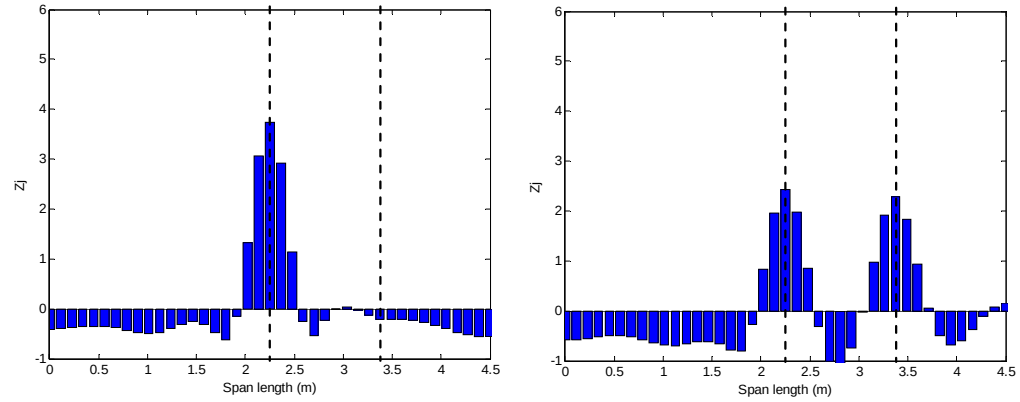

(a) 4S6L (b) 4S6S

Figure 5. Damage localization for two-damage cases

Damage Localization Results

In the following, results of damage localizations utilizing the MDI method are presented. MDI indices Z_j are calculated using the first five flexural modes. In the results, the damage localization indices for each of the damage cases are plotted against the beam span length. In principle, any location with the index value Z_j larger than zero (the probability-based criterion for damage detection) is considered as damage existing at that location. The actual damage locations are indicated with dashed line in all figures. In Figure 4, for single-damage cases, the MDI is able to indicate accurately the location of damage at position 2.25 m, with few false positives (indication of false damage locations) at position 0.5625 m, position 3.375 m and near the supports for case 4L. Figure 5 depicts the damage scenarios of two damage locations positioned at 2.25 m and 3.375 m detected with MDI. The severe damage at mid-span (4S) is precisely identified by the damage indicator in both cases. This also applies to the damage at position 3.375 m in damage case 4S6S, however, the light damage of damage case

4S6L stays undetected. It is shown that the MDI method is capable of detecting severe damage, but may miss out light damage that appears together with severe damage. This is due to light damage altering slightly the mode shape and its derivatives, which may have been overshadowed by other more severe scenarios. It is observed that damage index Z_j does change accordingly with increase severity of damage as seen in Figure 4. However, damage index Z_j (indication of probability of damage existence at the location j) is not capable of estimating the severity of damage.

Damage Severity Estimation Utilizing DI Method and ANN

Methodology of Quantitative Prediction of Damage

To enhance the severity assessment of the DI method, neural network techniques are introduced to the damage detection algorithm. A hierarchy of neural networks, referred to as neural network ensemble, are designed to estimate the loss of the second moment of area (I) of single damage cases. The damage estimator α_j of the DI method is used as input parameter to the networks. The α_j values of various vibrational modes have different characteristics and are of varying importance. To respect these differences and to generate well-prepared input data sets, the individual neural networks are trained with mode separated damage estimators. The network ensemble is first trained with data generated from finite element models of the timber beam, and then damage indices of the laboratory timber beam are fed to the ensemble to test the networks and to predict the damage severities. Three experimental damage cases are investigated. The cases are all situated at mid-span of the beam and are of severities L, M and S (4L, 4M and 4S), which correspond to a loss of "I" of 27.1%, 65.7%, and 87.5%, respectively. The mid-span location was chosen, as this is a node point of mode 2 and mode 4 and, therefore, most problematic for the DI method.

Artificial Neural Network Architecture

A neural network ensemble is designed to estimate damage severities of timber beam structures. Numerical beam stimulations are used to train the networks and experimental timber beam data are used to test the networks with previously unseen data. First, five individual neural networks are separately fed with α_j values of the first five flexural modes, and then the outputs of each of the networks are combined in an ensemble network to produce the final severity estimation. All networks in the ensemble are multi-layer perceptron neural networks. The individual neural networks comprise an input layer with 41 nodes, corresponding to the 41 data points of the severity estimator α_j; three hidden layers with 30, 20 and 10 nodes and one single node output layer estimating the severity of the damage. The network ensemble is designed with five input nodes, which are the outputs of the five individual networks; three hidden layers of 7, 5, and 3 nodes and one output node predicting the damage extent. The transfer functions used are hyperbolic tangent sigmoid functions. Training is performed utilizing the back-propagation conjugate gradient descent algorithm. The inputs are divided into three sets: a training, a validation and a testing set. While the network adjusts its weights from the training samples, its performance is supervised utilizing

the validation set to avoid overfitting. The network training stops when the error of the validation set increases while the error of the training set still decreases, which is the point when the generalization ability of the network is lost and overfitting occurs.

The complete data set of 35 numerical samples is allocated for training. For the laboratory beam data, the undamaged beam is experimentally tested five times, and the three damage cases are tested three times each. Thereby, a total of 45 α_j damage indices are generated (five undamaged data sets × three damaged data sets × three damage severity cases). The 45 experimental samples are divided into sets of 18 for validation and 27 for testing. The design and operation of all neural networks are performed with the software Alyuda NeuroIntelligence version 2.2 from Alyuda Research, Inc.

Damage Severity Results

In the following paragraph, the damage quantification predictions of the neural networks are presented. It is found that the results of the five individual networks greatly differ among each other. These prediction differences are a reflection of the individual characteristics of the different vibrational modes. In the subsequent figures, the horizontal-axis displays the 45 validation and testing samples of the three experimental damage cases 4L, 4M and 4S. The vertical-axis represents the normalized error, which is defined as $E_{norm}(d) = (T_d-O_d)/S_{max}$, where d is the damage case, T_d the target value, O_d the neural network predicted value and S_{max} the maximum severity (here, 100% loss of the second moment of area, "I"). Displayed in Figure 6 are the outcomes of the individual networks trained with the severity estimator α_j derived from (a) mode 2, (b) mode 3 and (c) mode 5. It is observed that the predictions of the network of mode 2 are incorrect for almost all damage cases. The reason for these errors is that for mode 2, the mid-span of the beam is a node point of flexural vibration and, therefore, the damage cannot be identified. For the network of mode 3, all medium and extra severe damage cases are below 10% normalized error; some large errors are obtained for extra-light damage. The network of mode 5 identifies all damage cases well with a maximum normalized error of 7.4%.

To determine the damage characteristics based only on the outcomes of the individual networks is problematic, as their damage predictions vary greatly. To achieve reliable damage identification, a conclusive, intelligent fusion of the network outcomes is necessary. This is achieved by the neural network ensemble, which combines the outcomes of the individual networks. Figure 7 displays the finial severity predictions of the ensemble network. It can be seen that the estimated severities of all damage cases eventually agree very well with the actual damage extents with a maximum normalized error of 4.4%. These results clearly show the effectiveness of the neural network ensemble approach, which produce results that are more accurate than any of the individual networks. These final predictions show that by introducing ANNs to the DI-based damage detection algorithm, shortcomings of the DI method, which was not able to quantify single light damage, can be overcome.

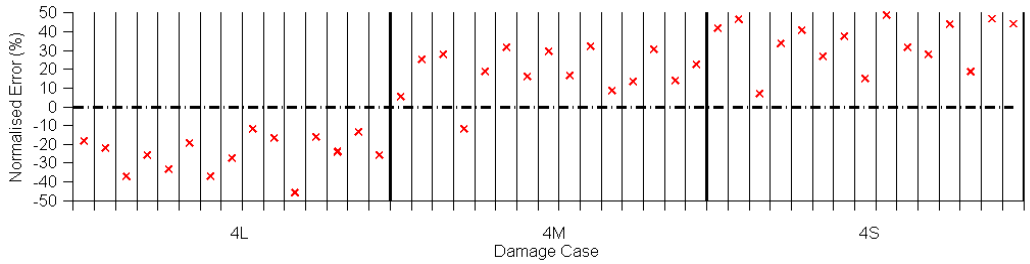

(a) Individual neural network outcomes trained with α_j derived from mode 2

(b) Individual neural network outcomes trained with α_j derived from mode 3

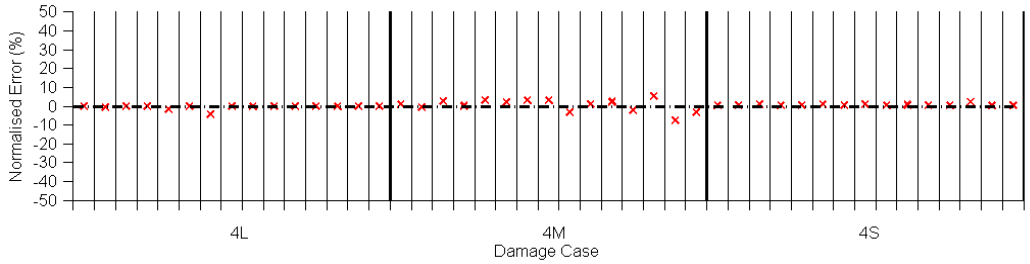

(c) Individual neural network outcomes trained with α_j derived from mode 5

Figure 6. Outcomes of individual neural networks tested with α_j damage indices derived from (a) mode 2, (b) mode 3 and (c) mode 5 to estimate the severity of experimental damage cases

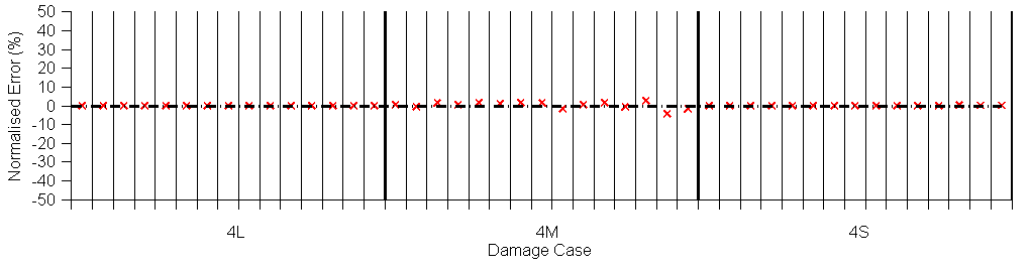

Figure 7. Final damage severity predictions of the neural network ensemble

DAMAGE DETECTION ON FOUR-GIRDER TIMBER BRIDGE

Four-Girder Laboratory Timber Bridge

A four-girder experimental timber bridge was built in the laboratory to verify the damage detection method for more complex timber structures. The basic dimensions of the deck structure are 2.4 m wide and 4.8 m long, with a span length of 4.5 m. The bridge was built of four girders (g1 to g4) of treated radiata pine sawn timber measuring 45 mm × 90 mm in cross-section. The deck consisted of four pieces of 21 mm thick × 2.4 m wide and 1.2 m long structural plywood of grade F11. The deck and girders were connected using 50 mm self-tapping screws with 137.5 mm spacing. No gluing was applied in order to avoid fully composite action, to simulate the interactions in a real timber bridge. The ends of the bridge girders were supported on concrete blocks and rigidly connected to the strong floor. A specially designed support system was used between girders and the concrete block to ensure a well-defined boundary condition that is very close to a pin-pin condition. The full bridge model is depicted in Figure 8. The goal of this study was to detect damage typically found in timber bridges. A total of 12 different damage scenarios at four damage locations were considered, as displayed in Figure 9. The inflicted damage cases consist of rectangular openings along the span of a girder starting from the soffit, located either at 1/8, 2/8, 4/8 (mid-span) or 6/8 of the span length to simulate pockets of rot. At each of these locations, three different damage severities were studied, denoted as light (“L”), medium (“M”) and severe (“S”) damage, respectively. All inflicted damage are 1% of the total span length (45 mm) and consist of 10%, 30% and 50% of the beam depth, corresponding to 27.1%, 65.7% and 87.5% loss of “I,” respectively. The three damage severities are shown in Figure 10. The damage cases were inflicted in a cumulative manner. First, damage was inflicted on girder 2 (g2), then on girder 4 (g4), subsequently on girder 3 (g3) and finally on girder 1 (g1).

Figure 8. The laboratory timber bridge

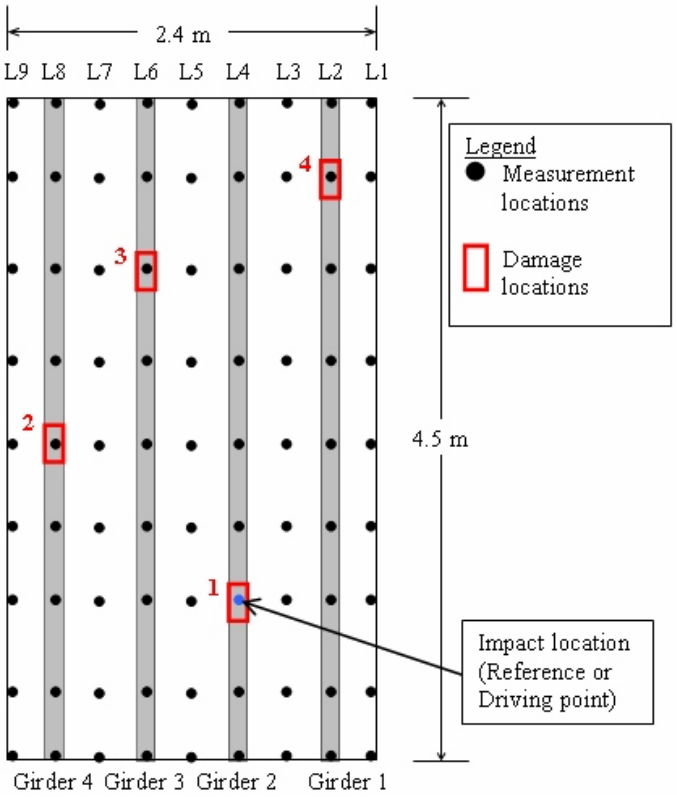

Figure 9. Plan view of damage and measurement locations on the bridge

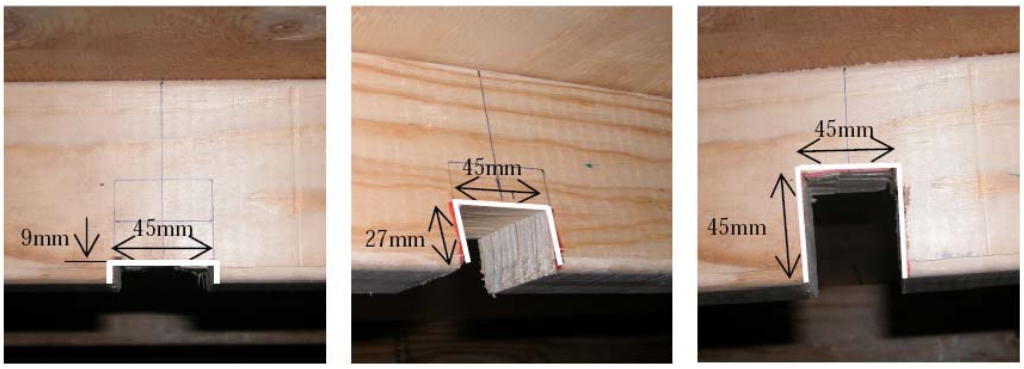

(a) Light damage (L) (b) Medium damage (M) (c) Severe damage (S)

Figure 10. Side view of various inflicted damage

Experimental Modal Analysis

The modal test set up and instrumentation layout is similar to the beam test as shown in Figure 2. However, the impact location (reference or driving point), which is situated at 3/4 of the span length and located directly above girder 2 (refer to Figure 9), is a strategic position

that excites a large number of modes simultaneously. The response signal along the span was recorded using nine piezoelectric accelerometers. For the entire bridge deck, data from 81 measuring points (depicted in Figure 9) were acquired. Due to the limited number of available sensors, the data acquisition for the 81 points was done in 9 tests. The nine non-stationary accelerometers were moved from line-to-line, i.e., from line 1 (L1) to line 9 (L9), until all measurement locations were covered. These accelerometers were used to measure the acceleration response on the top surface of the bridge. The nine measurement points per line were deemed sufficient for accurate reconstruction of mode shapes using interpolation techniques. The driving point measurement enabled the experimental mode shapes to be mass normalized. The captured mode shapes are shown in Figure 11. From the 9×9-point experimental mode shapes, 41×41-point mode shapes were reconstructed using two-dimensional (2-D) cubic spline interpolation technique, generating mode shape vectors with 41 coordinates in both longitudinal and transverse directions. The reconstructed mode shapes with finer coordinates have shown to provide better chance of locating damage compared to using coarse coordinates. The reconstructed mode shapes were then applied in the damage detection algorithms attempting to locate and evaluate the inflicted damage scenarios.

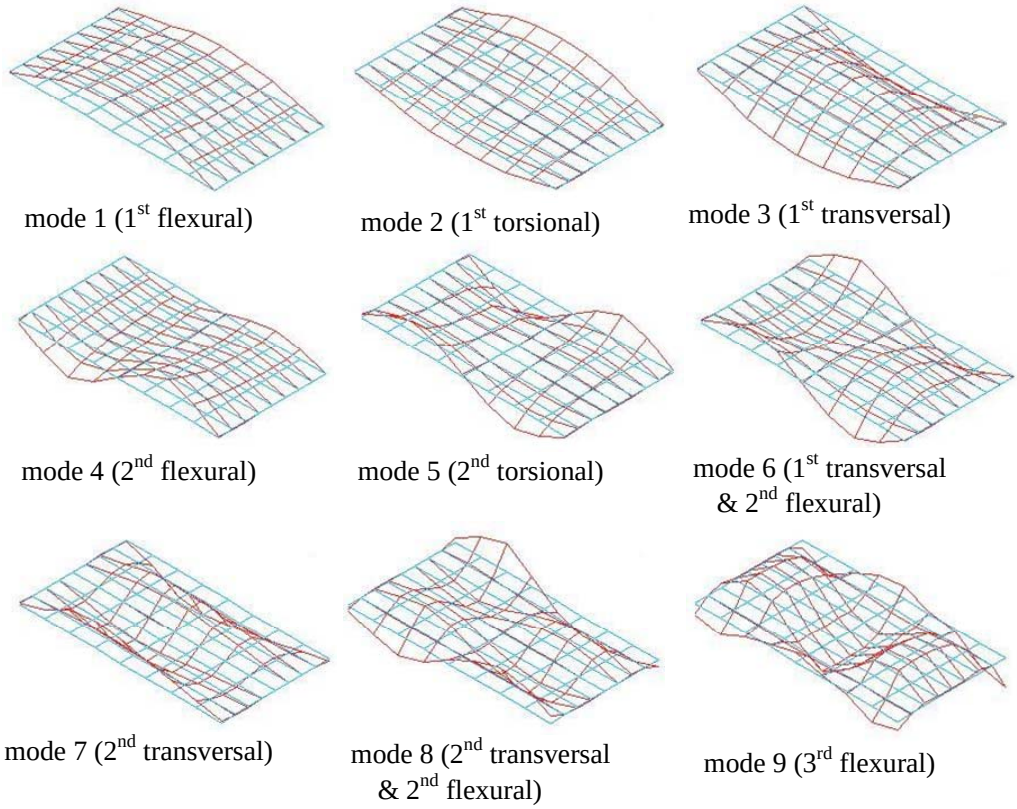

Figure 11. Experimental mode shapes (81-points) for the laboratory timber bridge

Damage Localization utilizing Damage Index for Plate-Like Structures (DI-P) for Bridge

Derivation of DI-P Method

Cornwell et al. (1999) extended the damage index method for beam-like structures to include the detection of damage for plate-like structures characterised by a two-dimensional (2-D) mode shape slope and curvature. The algorithm used to calculate the damage index for the jk^{th} subregion and the i^{th} mode, β_{ijk}, is given below for detecting the location of damage.

$$\beta_{ijk} = \frac{\left\{\int_{b_i}^{b_{j1}}\int_{a_i}^{a_{j1}}\left(\frac{\partial^2\phi_i^*}{\partial x^2}\right)^2+\left(\frac{\partial^2\phi_i^*}{\partial y^2}\right)^2+2\nu\left(\frac{\partial^2\phi_i^*}{\partial x^2}\right)\left(\frac{\partial^2\phi_i^*}{\partial y^2}\right)+2(1-\nu)\left(\frac{\partial^2\phi_i^*}{\partial x\partial y}\right)^2 dxdy\right\}\left\{\int_b^a\int\left(\frac{\partial^2\phi_i}{\partial x^2}\right)^2+\left(\frac{\partial^2\phi_i}{\partial y^2}\right)^2+2\nu\left(\frac{\partial^2\phi_i}{\partial x^2}\right)\left(\frac{\partial^2\phi_i}{\partial y^2}\right)+2(1-\nu)\left(\frac{\partial^2\phi_i}{\partial x\partial y}\right)^2 dxdy\right\}}{\left\{\int_{b_i}^{b_{j1}}\int_{a_i}^{a_{j1}}\left(\frac{\partial^2\phi_i}{\partial x^2}\right)^2+\left(\frac{\partial^2\phi_i}{\partial y^2}\right)^2+2\nu\left(\frac{\partial^2\phi_i}{\partial x^2}\right)\left(\frac{\partial^2\phi_i}{\partial y^2}\right)+2(1-\nu)\left(\frac{\partial^2\phi_i}{\partial x\partial y}\right)^2 dxdy\right\}\left\{\int_b^a\int\left(\frac{\partial^2\phi_i^*}{\partial x^2}\right)^2+\left(\frac{\partial^2\phi_i^*}{\partial y^2}\right)^2+2\nu\left(\frac{\partial^2\phi_i^*}{\partial x^2}\right)\left(\frac{\partial^2\phi_i^*}{\partial y^2}\right)+2(1-\nu)\left(\frac{\partial^2\phi_i^*}{\partial x\partial y}\right)^2 dxdy\right\}} \tag{5}$$

where ν represents Poisson's ratio, and the term $\partial^2\phi_t/\partial x^2$ is a vector of second derivatives of mode shape coordinates (curvatures) with respect to *x*-axis. Similar convention is applicable to second derivatives with respect to *y*-axis and cross derivatives with respect to *x*- and *y*-axes. Equation (5) denotes damage index in matrix form describing change of strain energy before and after damage, corresponding to mode *i* for a bridge structure. The asterisk denotes the damage cases. To account for all available modes, *NM*, the damage indicator value for a single subregion *jk* is given as

$$\beta_{jk} = \frac{\sum_{i=1}^{NM} Num_{ijk}}{\sum_{i=1}^{NM} Denom_{ijk}} \tag{6}$$

where Num_{ijk} = numerator of β_{ijk} and $Denom_{ijk}$ = denominator of β_{ijk} in Eq. (5), respectively. Transforming the damage indicator values into the standard normal space, the normalized damage index Z_{jk} is obtained

$$Z_{jk} = \frac{\beta_{jk} - \mu_{\beta_{jk}}}{\sigma_{\beta_{jk}}} \tag{7}$$

where $\mu_{\beta jk}$ = mean of β_{jk} values for all subregions *jk* and $\sigma_{\beta jk}$ = standard deviation of β_{jk} for all subregions *jk*. A judgment-based threshold value is again selected and used to determine which of the subregions *jk* are possibly damaged.

Damage Localisation Results

In the following, the normalized damage indicator, Z_{jk}, calculated from the first nine modes is plotted against the laboratory timber bridge span length (4.5 m) and width (2.4 m). In principle, when the statistically normalized damage indicator value of Z_{jk} for a given

location is larger than or equal to two (the probability-based criterion for damage), it is considered that damage exists at that location. To show the damage site in the contour plots, the actual damage locations are marked by an arrow sign and labeled with “Damage” in all subsequent figures.

The damage localization results of single damage cases are illustrated in Figure 12. For the light damage case g2L (the smallest damage), depicted in Figure 12(a), the method could not locate the damage at position (3.375 m, 0.9 m). For the severe damage case g2S, which is illustrated in Figure 12(b), the damage location was clearly detected, even though there were some false positives.

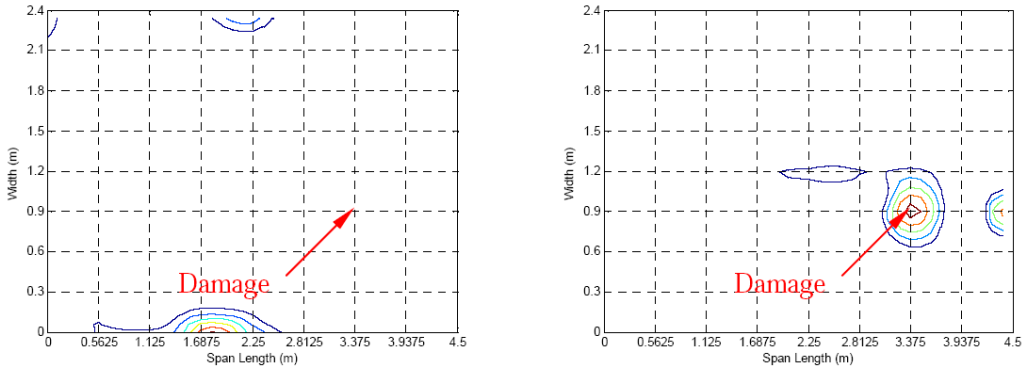

(a) g2L (b) g2S

Figure 12. Single-damage cases using the experimental data

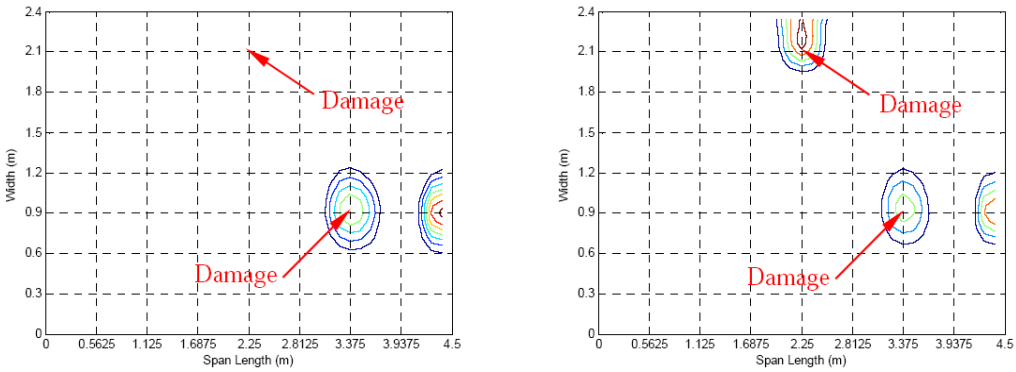

(a) g2Sg4L (b) g2Sg4S

Figure 13. Two-damage cases using the experimental data

Observing from the results in Figure 13, severe damage locations at position (3.375 m, 0.9 m) were identified for damage cases g2Sg4L and g2Sg4S (see Figure 13(a) and (b), respectively) as well as severe damage at position (2.25 m, 2.1 m) for case g2Sg4S. However, the light damage at position (2.25 m, 2.1 m) was not identified for case g2Sg2L. A possible explanation is that the change in mode shape curvature caused by the severe damage is dominating the results and overwhelming the curvature change due to the light and medium

damage. From the two damage cases, it should be noted that the second damage at position (2.25 m, 2.1 m) was not detected until this damage became roughly comparable in severity to the first severe damage at position (3.375 m, 0.9 m) in the experimental studies. This indicates that the method may encounter problems in identifying multiple damage locations with different degrees of severity using experimental data. However, the method is capable of identifying all severe damage locations, and this is critical for a structure in terms of avoiding catastrophic failure. Detecting less severe damage in timber bridges using this method can be achieved as a two-stage process. Once the severe damage is identified and repaired, the method can be applied again and then any less severe damage can be detected in the absence of any severe damage. A detailed discussion on the assessment of all investigated timber bridge damage cases with the DI-P method can be found in Choi (2007).

Damage Severity Assessment Utilizing Frequency Response Functions and ANN

Methodology of Severity Detection

The DI-P method does not provide an algorithm for the estimation of damage severity. A different dynamic approach based on frequency response functions (FRFs) and artificial neural networks was developed to quantitatively estimate defects. FRF data are directly measured data, which have an abundance of information. They are easy to obtain and require very little human involvement (Fang and Tang, 2005). However, a very significant obstacle is the large size of the FRF data. Utilizing full-size FRFs in neural networks will result in a large number of input nodes, which will cause problems in training convergence and computational efficiency. If only partial sets of FRF data are used, an improper selection of data points from frequency windows will result in loss of important information, and errors will be introduced to the detection scheme (Ni et al., 2006). Principal Component Analysis (PCA) is a statistical technique for achieving dimensional data reduction and feature extraction. By projecting data onto the most important principal components, its size can greatly be reduced without significantly affecting the data. In the developed method, PCA is employed to compress the size of FRF data and make them suitable for network training. More precisely, residual FRFs, which are differences in FRF data between baseline and damage state, are compressed and used as ANN input. To demonstrate the method, it is applied to the different damage stages of the laboratory timber bridge. An accumulative damage growth, as simulated in the experimental bridge structure, is a common condition in field bridges. Unfortunately, in many circumstances, data on the intact state of these structures are not available. However, it is of importance for road engineers to obtain information on possible advancements of existing (even though unknown) damages as well as on newly acquired defects. To consider these needs, in this study, four different stages related to the four damage locations of the timber bridge are investigated. In the first stage, the undamaged structure is considered to be the baseline state, and the progress of damage at girder 2 is analyzed. In the second stage, the most severe damage case at girder 2 is regarded as baseline and the progress of damage at girder 4 is examined. In the third stage, the largest damage extent of damage at girder 4 (and the already existing damage at girder 2) is baseline and damage at girder 3 is investigated. Finally, the biggest damage state at girder 3 (including damage at girder 2 and 4) constitutes the baseline state and the extents of damage stages at

girder 1 are analyzed. On each girder, nine accelerometer measurements are available. To minimize the effort for neural network training, the FRF data of the nine accelerometers of each girder are added up to obtain one summation FRF for each girder and each damage state. These summation FRFs are the bases for the network training.

Artificial Neural Network Architecture

Four neural networks are created utilizing the NeuroIntelligence software from Alyuda to estimate the severities of damage at girders 1 to 4. Each network is trained independently with data derived from summation FRFs of the four girders. First, differences in summation FRF data between the baseline state and the damage state are calculated. Then, PCA techniques are adopted to compress the residual FRFs onto its most important principal components. The PCA-compressed residual FRFs are then separated by girders and fed to the four neural networks to estimate the severity of damage. The created networks are back-propagation neural networks utilizing hyperbolic tangent sigmoid transfer functions and conjugate gradient descent training algorithms. The networks comprise of an input layer of nine nodes, representing the number of the selected PCs (the first nine principal components account for 97% of the original data); five hidden layers of 10, 8, 6, 4 and 2 nodes and one single node output layer estimating the extent of the damage. As each damage state is tested three times, a total of 108 data sets are available (three baseline data sets × three damaged data sets × four damage locations × three damage severities). The input set is again divided into a training, a validation and a testing set of 60, 24 and 24 data samples, respectively.

Damage Severity Outcomes

The damage severity estimations of the four neural networks are very promising. Each of the networks trained with measurements from one of the four bridge girders predicts the severity level of all 108 damage samples correctly. The outcomes of the network trained with PCA-compressed residual FRFs of girder 1 are displayed in Figure 14. These results show that damage fingerprints in FRF data are very good indicators for quantitatively estimating damage extents. As the predictions of each network give independently precise damage detections, a reduction of the sensor network is possible. Data from only nine sensors of one girder (or even less) are enough to successfully assess the severities of accumulative damage in the studied laboratory timber bridge.

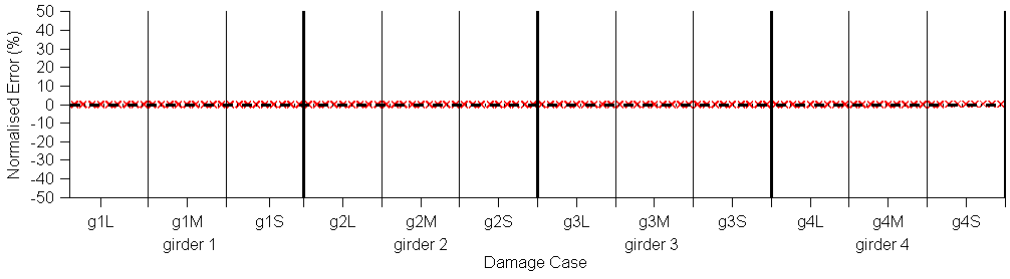

Figure 14. Outcome of neural network trained with PCA-compressed residual FRFs of girder 1

DETERMINATION OF EMBEDMENT DEPTH OF TIMBER POLE

Background of Research

Different types of non-destructive evaluation (NDE) techniques were developed during the last decades and used to evaluate the embedment depth and the quality of materials of embedded structures such as concrete piles. Some of these tests have also been utilized on timber piles or poles. However, the extent of knowledge developed on NDE techniques for timber poles and piles appears to be inadequate, but the effectiveness and reliability of the NDE techniques are not often questioned.

An ongoing research project of the Centre for Built Infrastructure Research (CBIR) at the University of Technology Sydney is the investigation on adequacy of the current NDE techniques for estimation of underground depth and condition of in-service timber pole structures as well as development of a new reliable and robust technique. The first stage of this research aims at conducting comprehensive state-of-the-art evaluations on available NDE techniques in terms of the reliability and effectiveness through numerical and experimental investigations. In the second stage, a new vibration- and acoustic-based NDE technique and procedure will be developed to encompass the latest development on advanced signal processing and damage detection, and to provide a reliable and effective tool for determination of the depth of embedment of timber poles/piles as well as their in-service condition including damage identification.

The current state-of-practice for non-destructive determination of unknown condition and embedded length of poles or piles are generally stress-wave-based and can be divided into two groups: the surface NDT methods and the borehole NDT methods. In the surface NDT, the reflection of the stress wave is measured directly from the pole/pile, while in the borehole methods, it needs a borehole drilled close to the pole/pile and extends along its length to perform tests. In this case, the reflection is monitored in the borehole. The potential applications of surface NDE techniques for pole or pile depth determination are Sonic Echo/Impulse Response (compressional wave generated from longitudinal impulse), Bending Wave (dispersive wave generated from transverse impulse), and Ultraseisminc Vertical Proofing with geophysical processing of the data (compressional and flexural wave). Borehole NDE techniques include Parallel Seismic, i.e., direct measurement of compressional and shear wave arrival to receivers in a borehole emitted by wave travelling down the pile from an impact to the exposed substructure, Borehole Radar, i.e., reflection of electromagnetic wave energy is measured from nearby substructure.

The research has mainly been focused on surface wave methods to meet the time- and cost-effective requirements of the project.

Experimental Investigations

A number of tests have been conducted, including investigations into suitable hardware (such as data acquisition system and cost-effective sensors), stress wave patterns, reliability and uncertainty issues. Three types of columnar specimens have been used in the current investigations, i.e., a 5 m steel RHS beam, a 5 m rectangular timber beam and a 5 m timber

pole. Considering the uncertainty on the material property of timber, a steel beam, consisting of homogeneous material without defects, was chosen as benchmark material for all stress wave tests. The rectangular timber beam without any defects was used to verify the behaviour of "ideal" timber during tests. Several timber poles taken out of service and containing local defects and uncertainty on its properties, have been used as "real" pole specimens.

To be able to simulate geological embedment conditions for field specimens, a container, 1.2m × 1.2m in cross-section and three meters in height has been designed and fabricated to contain sand/soil for embedding different type of specimens (see Figure 15(b) and (c)). Fully instrumented benchmark specimens and pole specimens are then embedded, up to three meters, into the foundations consisting of eight layers of sand/soil. Various NDE techniques are then conducted on embedded specimens. The length of embedment can also be changed during the tests by simply pulling the specimens up and compacting sand/soil. Underground or embedded portion of the specimens were also instrumented so that stress wave patterns can be tracked down. Figure 15(a) shows the schematic NDE test set up under embedded conditions.

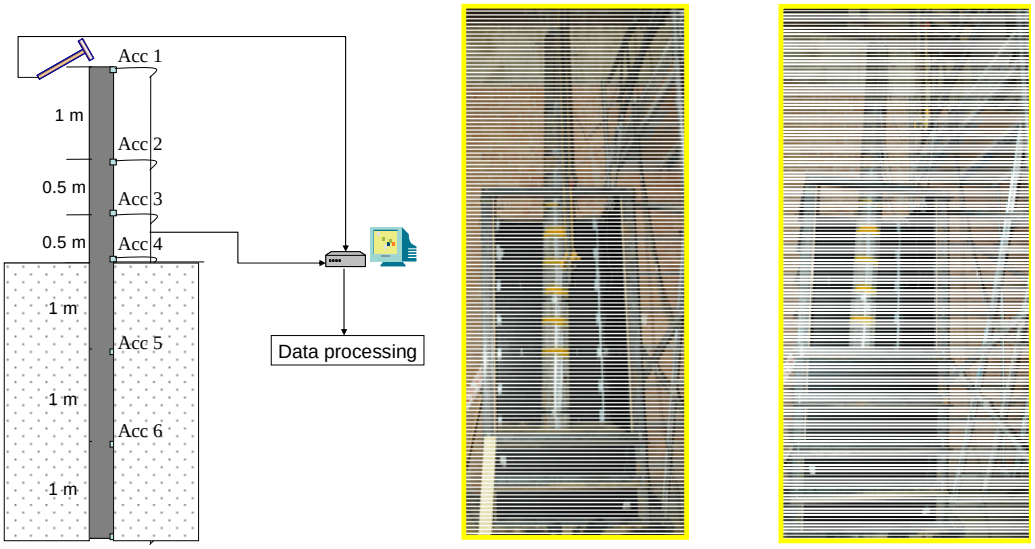

(a) Schematic NDE test set up (b) Embedded depth 0.8m (c) Embedded depth 1.6m

Figure 15. The laboratory set-up for NDT test on embedded depth and condition of timber pole

A set of typical results from a longitudinal stress wave test of a timber pole are shown in Figure 16. Results show measured acceleration time histories and calculated velocity after the filtration from six sensors along the length of the pole. Using different techniques, length and condition of the pole can be estimated.

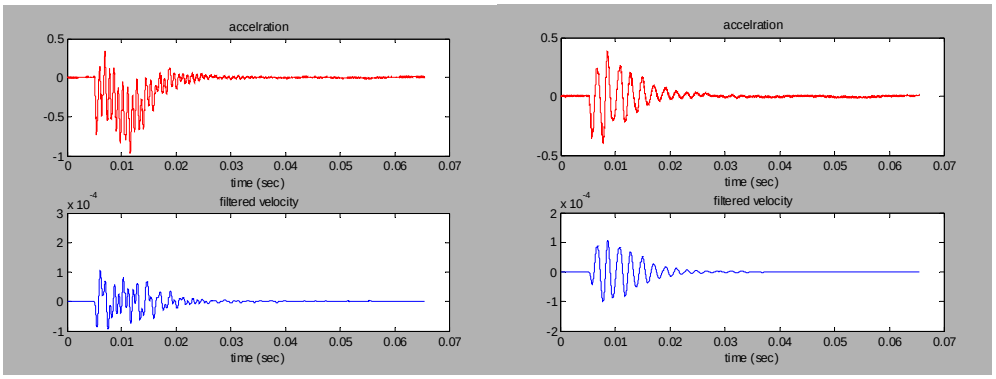

(a) Accelerometer 1 (Acc 1) (b) Accelerometer 2 (Acc 2)

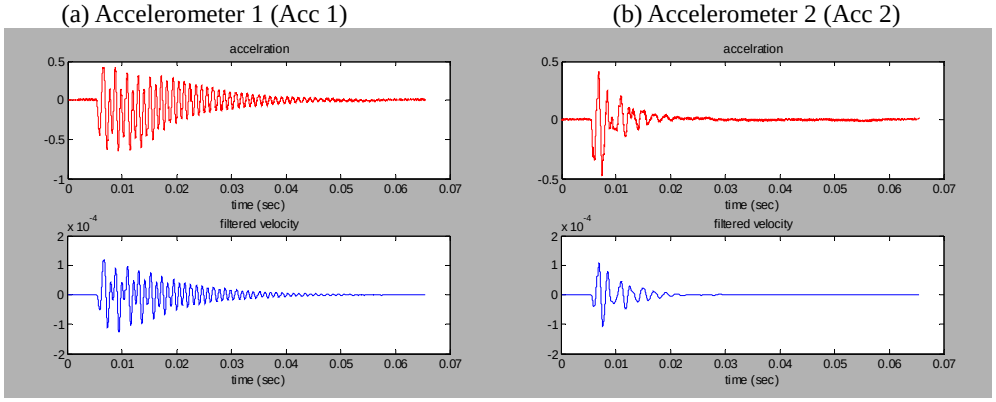

(c) Accelerometer 3 (Acc 3) (d) Accelerometer 4 (Acc 4)

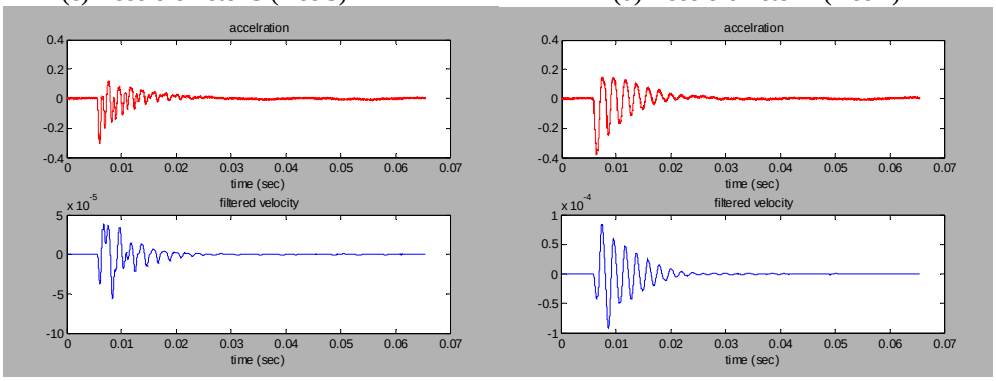

(e) Accelerometer 5 (Acc 5) (f) Accelerometer 6 (Acc 6)

Figure 16. Acceleration and velocity obtained from a timber pole stress wave test

CONCLUSION

This chapter presents research work on vibration-based damage detection methods of timber structures. The developed damage identification procedures are verified by two laboratory structures, a simple timber beam and a laboratory timber bridge deck. A modified damage index (MDI) method was proposed to locate damage in the timber beam structures. The method utilizes the first five mode shapes of the structure and their derivatives obtained

from experimental modal analysis. The results showed that the modified algorithm is effective and reliable in locating damage, even though it comes with some false positives. For severity assessment, ANNs are introduced to compensate the shortcoming of the method to quantify severity of damage in the timber beam. The severity estimator of the DI method is used as an input parameter to a neural network ensemble. The individual networks of the ensemble are trained with modally separated severity estimators in order to take advantage of distinguishable patterns of different vibrational modes and thereby to increase efficiency of network training and produce more accurate and robust damage detection results. The outcomes showed that the severities of all damage cases can be successfully determined by the network ensemble. Further, it was shown that the network ensemble produced more accurate predictions than any of the individual networks.

For the laboratory timber bridge, the research proposed the DI-P method for damage location identification. The method uses the first nine modes obtained from experimental modal analysis to locate single- and multiple-damage in the structure. The locations of all severe damage cases in the single- and the two-damage scenarios can be successfully identified. However, light- and medium-damage cases could not be located reliably. To evaluate the severity of damage in the timber bridge, compressed residual FRFs were proposed and used as damage indicator for neural network inputs. Neural networks were then trained with the FRF-based damage fingerprints to predict the severity of accumulative damage cases. The results showed that for all damage cases, even those of light severity, of the laboratory timber bridge, the proposed neural network ensemble was able to identify the level of damage severity reliably.

As an example, the chapter also introduced current research on determination of in-service condition and embedment depth of timber poles using NDE techniques, including some testing set-up and initial results of experimental investigation.

ACKNOWLEDGEMENTS

The authors wish to thank the Centre for Built Infrastructure Research (CBIR), the School of Civil and Environmental Engineering, University of Technology Sydney for supporting this work. The authors would like to thank Prof. Keith Crews for contributing his expertise and experiences in many aspects of this study. Finally, the authors wish to render thanks to staff of UTS Structures Laboratory for their assistance in conducting the experimental works.

REFERENCES

Bakhary, N., Hao, H., Deeks. A. J. (2007) "Damage Detection Using Artificial Neural Network with Consideration of Uncertainties." *Engineering Structures*. 29(11) pp. 2806-2815.

Benitez, M.F. and Li, J. (2002) "Static and Dynamic Evaluation of A Timber Bridge (Cattai Ck. Bridge NSW, Australia)." *Proceedings of the 7th World Conference on Timber*

Engineering. (WCTE 2002), 12-15 August, 2002 Shah Alam, Selangor, Malaysia, pp. 385-393.

Choi, F. C., Li, J., Samali, B. and Crews, K. (2007) "Application of Modal-based Damage Detection Method to Locate and Evaluate Damage in Timber Beams." *Journal of Wood Science*. 53(5) pp. 394-400.

Choi, F. C. (2007) *Assessment of the Structural Integrity of Bridges Using Dynamic Approaches*: PhD Thesis: Faculty of Engineering: University of Technology Sydney: Australia.

Choi, F. C., Li, J., Samali, B. and Crews, K. (2008a) "Application of the Modified Damage Index Method to Timber Beams." *Engineering Structures*. 30(4) pp. 1124-1145.

Choi, F. C., Li, J., Samali, B. and Crews, K. (2008b) "An Experimental Study on Damage Detection of Structures using a Timber Beam." *Journal of Mechanical Science and Technology - MOVIC Special Edition*. 21(6) pp. 903-907.

Cornwell, P. J., Doebling, S. W. and Farrar, C. R. (1999) "Application on the Strain Energy Damage Detection Method to Plate-like Structures." *Journal of Sound and Vibration*. 224(2) pp. 359-374.

Crews, K. (2008) "An Overview of the Development of On-site Assessment for Timber Structures in Australia." *Proceedings of the International RILEM conference - On Site Assessment of Concrete, Masonry and Timber Structures.* (SAComaTiS 2008), 1-2 September, 2008 Varenna, Italy, pp. 1113-1124.

Crews, K., Samali, B., Bakoss, S. and Champion, C. (2004) "Overview of Assessing the Load Carrying Capacity of Timber Bridges Using Dynamic Methods." *Proceedings of the 5th Austroads Bridge Conference*, 19-24 May, 2004 Tasmania, Australia, (published on CD-ROM).

Dackermann, U., Li, J., Samali, B., Choi, F. C. and Crews, K. (2008a) "Experimental Verification of a Vibration-Based Damage Identification Method in a Timber Structure Utilizing Neural Network Ensembles." *Proceedings of the International RILEM conference - On Site Assessment of Concrete, Masonry and Timber Structures.* (SAComaTiS 2008), 1-2 September, 2008 Varenna, Italy, pp. 1049-1058.

Dackermann, U., Li, J., Samali, B., Choi, F. C. and Crews, K. (2008b) "Vibration-Based Damage Identification in Civil Engineering Structures utilizing Artificial Neural Networks." *Proceedings of the 12th International Conference on Structural Faults and Repair*. 10-12 June, 2008 Edinburgh, Scotland, (published on CD-ROM).

Dackermann, U., Li. J. and Samali, B. (2009) "Vibration-based Damage Identification in Timber Structures Utilizing the Damage Index Method and Neural Network Ensembles." *Australian Journal of Structural Engineering*. 9(3) pp. 181-194.

DoTaRS (Department of Transport and Regional Services) (2003) *2002-03 Report on the Operation of the Local Government (Financial Assistance) Act 1995*: Canberra: Commonwealth of Australia.

Duwadi, S. R., Ritter, M. A. and Cesa, E. (2000) "Wood in Transportation Program: An Overview." *Fifth International Bridge Engineering Conference*. 3-5 April, 2000, Tampa, Florida, US, pp. 310-315.

Fang, X. and Tang, J. (2005) "Frequency Response Based Damage Detection Using Principal Component Analysis." *Proceedings of the 2005 IEEE International Conference on Information Acquisition*. 27 June-3 July, 2005 Hong Kong and Macau, pp.407-412.

Francis, L. and Narton, J. (2006) *Australian Timber Pole Resources for Energy Networks`- A Review*: Report: Department of Primary Industries and Fisheries: Queensland.

Hu, C. and Afzal, M. T. (2006) "A Statistical Algorithm for Comparing Mode Shapes of Vibration Testing Before and After Damage in Timbers." *Journal of Wood Science*. 52(4) pp. 348-352.

Kasal, B. (2008) "In Situ Evaluation of Timber Structures- Education, State-of-the-art and Future Directions." *Proceedings of the International RILEM conference - On Site Assessment of Concrete, Masonry and Timber Structures.* (SAComaTiS 2008), 1-2 September, 2008 Varenna, Italy, pp. 1025-1032.

Kim, J.-T. and Stubbs, N. (1995) "Model-Uncertainty Impact and Damage-Detection Accuracy in Plate Girder." *Journal of Structural Engineering.* 121(10) pp. 1409-1417.

Ko, J. M., Sun, Z. G. and Ni, Y. Q. (2002) "Multi-stage Identification Scheme for Detecting Damage in Cable-stayed Kap Shui Mun Bridge." *Engineering Structures*. 24(7) pp. 857-868.

Lee, J. J. and Yun, C. B. (2006) "Damage Diagnosis of Steel Girder Bridges Using Ambient Vibration Data." *Engineering Structures.* 28(6) pp. 912-925.

Li, J., Choi, F. C., Samali, B. and Crews, K. (2007) "Damage Localization and Severity Evaluation of A Beam-like Timber Structures Based on Modal Strain Energy and Flexibility Approaches." *Journal of Building Appraisal.* 2(4) PP. 323-334.

Li, J., Samali, B. and Crews, K. I. (2004) "Determining Individual Member Stiffness of Bridge Structures Using a Simple Dynamic Procedure." *Acoustics Australia*. 32(1) pp. 9-12.

Li, J., Samali, B., Crews, K., Choi, F. and Shestha, R. (2005) "Theoretical and Experimental Studies on Assessment of Bridges Using Simple Dynamic Procedures." *Proceedings of the 2005 Australian Structural Engineering Conference - Structural Engineering - Preserving and Building into the Future.* (ASEC 2005), 11-14 September, 2005 Newcastle, New South Wales, Australia, (published on CDROM).

Marwala, T. and Hunt, H. E. M. (1999) "Fault Identification Using Finite Element Models and Neural Networks." *Mechanical Systems and Signal Processing*. 13(3) pp. 475-490.

Marwala, T. (2002) "Damage Identification Using Committee of Neural Networks." *Journal of Engineering Mechanics*.126(11) pp. 43-50.

McInnes, K (2005) *Conserving Historic Timber Bridges*: National Trust of Australia: Victoria.

Morison, A., VanKarsen, C. D., Evensen, H. A., Ligon, J. B., Erickson, J. R., Ross, R. J. and Forsman, J. W. (2002) "Timber Bridge Evaluation: A Global Nondestructive Approach Using Impact Generated FRFs." *Proceedings of the 20th International Modal Analysis Conference.* (IMAC-XX 2002), 4-7 February, 2002 Los Angeles, California, US, pp. 1567-1573.

Morison, A., VanKarsen, C. D., Evensen, H. A., Ligon, J. B., Erickson, J. R., Ross, R. J. and Forsman, J. W. (2003) "Dynamic Characteristics of Timber Bridges as A Measure of Structural Integrity." *Proceedings of the 21st International Modal Analysis Conference.* (IMAC-XXI 2003), 3-6 February, 2003 Kissimme, Florida, US, (published on CD-ROM).

Muller, W. (2008) "GPR Inspection of the World's Longest Timber Bridge." *Proceedings of the 12th International Conference on Structural Faults and Repair*. 10-12 June, 2008 Edinburgh, Scotland, (published on CD-ROM).

Nguyen, M., Foliente, G. and Wang, X. (2004) “State of the Practice and Challenges in Non-destructive Evaluation of Utility Poles in Service.” *Key Engineering Materials Journal – Advances in Non-destructive Evaluation*. Transportation Technology Publications 270-273 pp. 1521-1528.

Ni, Y. Q., Zhou, X. T. and Ko, J. M. (2006) "Experimental Investigation of Seismic Damage Identification Using PCA-compressed Frequency Response Functions and Neural Networks." *Journal of Sound and Vibration*. 290(1-2) pp. 242-263.

Perrone, M. P. and Cooper, L. N. (1993) "When Networks Disagree: Ensemble Methods for Hybrid Neural Networks." *Artificial Neural Networks for Speech and Vision*: Chapman and Hall: London.

Peterson S. T., McLean, D. I., Symans, M. D., Pollock, D. G., Cofer, W. F., Emerson, R. N. and Fridley, K. J. (2001a) "Application of Dynamic System Identification to Timber Beams I." *Journal of Structural Engineering*. 127(4) pp. 418-425.

Peterson S. T., McLean, D. I., Symans, M. D., Pollock, D. G., Cofer, W. F., Emerson, R. N. and Fridley, K. J. (2001b) "Application of Dynamic System Identification to Timber Beams II." *Journal of Structural Engineering*. 127(4) pp. 426-432.

Ross, R. J., Brashaw, B. K. and Wang, X. (2006) "Structural Condition Assessment of In-service Wood." *Forest Products Journal*. 56(6) pp. 4-8.

Sahin, M. and Shenoi, R. A. (2002) "Quantification and Localization of Damage in Beam-like Structures by Using Artificial Neural Networks with Experimental Validation." *Engineering Structures*. 25(14) pp. 1785-1802.

Samali, B., Bakoss, S. L., Crews, K. I., Li, J. and Champion, C. (2002) "Assessing the Load Carrying Capacity of Timber Bridges Using Dynamic Methods." *IPWEA Queensland Division Annual Conference*. 23 October, 2002 Noosa, Queensland, Australia, (published on CD-ROM).

Samali, B., Bakoss, S. L., Li, J., Saleh, A. and Ariyaratne, W. (2003a) "Assessing the Structural Adequacy of A 3-span Steel-concrete Bridge using Dynamic Methods: A Case Study." *Proceedings of the 10th International Conference: Structural and Faults and Repair*. 1-3 July, 2003. London, UK, (published on CD-ROM).

Samali, B., Crews, K. I., Li, J., Bakoss, S. L. and Champion, C. (2003b) "Assessing the Load Carrying Capacity of Timber Bridges Using Dynamic Methods." *IPWEA Western Australia State Conference*. 7 March, 2003 Perth, Western Australia, Australia, (published on CD-ROM).

Samali, B., Li, J., Choi, F. C. and Crews, K. (2009) "Application of the Damage Index Method for Plate-like Structures to Timber Bridges." *Structural Control and Health Monitoring*. (Published online 8-July-2009 in Wiley Interscience, *DOI: 10.1002/stc.347*).

Wang, X., Wacker, J. P., Morison, A. M., Forsman, J. M., Erickson, J. R. and Ross, R. J. (2005) *Nondestructive Assessment of Single-span Timber Bridges using A Vibration-based Method*: Research Paper FPL-RP-627: Madison: Forest Products Laboratory.

Wu, X., Ghaboussi, J. and Garrett, J. H. Jr. (1992) "Use of Neural Networks in Detection of Structural Damage." *Computers and Structures*. 42(4) pp. 649-659.

Zad, A. (2009) *Doctoral Assessment Report*: Faculty of Engineering and IT: University of Technology Sydney: Australia.